

Fabrication of Activated Carbon Pouch Cell Supercapacitor: Effects of Calendering and Selection of Separator-Solvent Combination

Gladis Aros Safitri¹, Khanin Nueangnoraj¹, Paiboon Sreearunothai¹ and
Jedsada Manyam^{2*}

¹School of Bio-Chemical Engineering and Technology, Sirindhorn International Institute
of Technology (SIIT), Pathum Thani, Thailand

²National Nanotechnology Center (NANOTEC), National Science and Technology
Development Agency (NSTDA), Pathum Thani, Thailand

Received: 11 September 2019, Revised: 8 December 2019, Accepted: 9 January 2020

Abstract

Most published articles reported characterization of a supercapacitor utilizing a coin cell or a Swagelok cell design, while the higher capacity format such as a pouch or cylindrical cell is needed to predict the performance of a supercapacitor for a practical application. In this work, the guideline to produce a pouch cell supercapacitor is given. The three-component electrode is based on a commercially available activated carbon, carbon black, and a polyvinylidene fluoride binder, which is formed a layer on a conductive-carbon coated aluminum foil current collector. The roles and optimization of a calendering process and selection of a separator-solvent combination are highlighted. The symmetric electric double-layer capacitor (EDLC) pouch cell using organic salt electrolyte is rated at 2.5 Volt. The pouch cell has the maximum capacitance of 32.6 F with a specific capacitance of 25.6-29.4 F/g.

Keywords: supercapacitor, pouch cell, electric double-layer capacitor (EDLC), activated carbon, organic electrolyte

DOI 10.14456/cast.2020.2

1. Introduction

The foreseeable limit of fossil fuel reserves, accompanied with an increasing concern about environmental impacts, initiates the development of alternative technologies that promote the efficient use of energy and renewable sources. However, the implementation of grid-scale electricity generated from renewable sources requires grid balancing to compensate for an intermittency issue in which energy storage technologies could play a crucial role [1]. In addition, a recent trend in the penetration of electric vehicles (EV) is another driver of growing demand on the advancement of high energy and power density storage devices [2]. Li-ion batteries and supercapacitors are among the potential storage technologies which have received increasing attention in the past few years for both stationary and transportation applications [2-5].

*Corresponding author: E-mail: jedsada@nanotec.or.th

Although a Li-ion battery is preferable as a primary power source in mainstream design due to its high energy density (~200 Wh/kg) and cost effectiveness, supercapacitor which possesses relatively high power density (~10 kW/kg) and extremely long life cycle can find its niche applications such as a power source for the EV regenerative braking and a blade pitch control in wind turbine generator [2, 6, 7]. In addition, a battery and a supercapacitor could be integrated to provide robust energy management [2, 8].

A supercapacitor electrode stores polarization energy in an electric double-layer built up by the accumulation of ions and electric charges near the interface between a highly porous electrode and an electrolyte solution without having an electron transfer reaction, providing the fast charge-discharge rate. It is also widely known as an electric double-layer capacitor (EDLC). The design of EDLC involves the selection of electrode materials, electrolytes and separators. The selection of components can be the first consideration to minimize the trade-off between the electrode performance and the material cost. A commercially available EDLC uses activated carbon as an electrode material because of its high specific surface area (up to 3,000 m²/g), good electrical conductivity, excellent chemical stability and low cost [9]. In a typical electrode formulation, carbon black and a thermoplastic binder are added to improve electrical conductivity and adhesion, respectively [10, 11]. An organic electrolyte such as tetraethylammonium tetrafluoroborate (TEABF₄) in an organic solvent is commonly used in a commercial cell because it provides moderate ionic conductivity and relatively high voltage rating, typically 2.7 V, and the larger amount of energy stored in comparison to an aqueous electrolyte system [12]. A separator, commonly made of a porous sheet of polyolefins, glass, or cellulose, serves as an insulating layer to prevent electrical contact between a negative electrode and a positive electrode. It must possess high porosity and good wettability to be able to absorb and retain electrolyte which supports sufficient ionic conductivity and interfacial contact to electrode surface [13, 14].

Apart from a material aspect, the performance of a supercapacitor cell indicated by capacitance and internal resistance can be significantly varied by a number of factors regarding electrode processing conditions and a cell assembly such as thickness [15] and density [16, 17] of an electrode, cell pressure [18], and pre-conditioning process [19]. A brief fabrication process for a supercapacitor includes (1) preparation of a homogeneous mixture of ingredients, (2) forming an electrode layer on a sheet of a current collector, (3) cell assembling, and (4) packaging. In a laboratory, a pair of small electrodes, a few cm² area or mF capacity, are normally packed in a coin cell or other derivatives such as a Swagelok cell in order to characterize an electrode material in a full cell configuration. However, demonstration of a large capacity cell is needed to evaluate the cell performance in a practical aspect and it is also the step toward commercialization. A high capacity cell, 10s-1000s F, requires packaging in a cylindrical or pouch cell. Unfortunately, the guideline to produce a cell in such large package is proprietary in the industrial domain and a little information is provided in the published research. An attempt to scale up the size of a supercapacitor coin cell to a larger format, specifically a pouch cell, has been recently reported, pointing out a challenge on electrode preparation and processing [17, 19-21]. The pouch cell packaging seems the preferable format in literature because of its simplicity, affordable processing, industrial compatibility as well as design of the minimum footprint.

In this paper, we report prototyping of a 30-farad EDLC pouch cell made of commercially available materials. The basic instructions for the preparation of a carbon-based electrode and a pouch cell package are described. The roles of the calendaring process, which governs the thickness and density of an electrode and the selection of a separator-solvent system to the electrode performance is highlighted and discussed. The process optimization and the characterization of the as-fabricated pouch cells are reported.

2. Materials and Methods

2.1 Electrode preparation

All chemicals were commercially available and reagent grade, unless otherwise stated. A supercapacitor-grade activated carbon powder was purchased from TOB (China) having a Brunauer-Emmett-Telle (BET) specific surface area of $1,894 \text{ m}^2/\text{g}$. A carbon black Super-P (TOB, China) was used as a conductive agent. A binder was polyvinylidene fluoride (PVdF; Sigma Aldrich, Germany). Three different separators were tested in this study: (1) A $180\text{-}\mu\text{m}$ thick cellulose Whatman filter paper (grade 1) was used only for an aqueous electrolyte system in a Swagelok test cell, (2) A $35\text{-}\mu\text{m}$ thick cellulose NKK TF4035 separator (Nippon Kodoshi, Japan), having 75% porosity [22] and (3) A $25\text{-}\mu\text{m}$ thick polypropylene (PP) separator (TOB, China). The porosity of a PP separator is specified to be 43.5% [23]. A current collector was $15\text{-}\mu\text{m}$ -thick aluminum foil having a thin layer of conductive coating (TOB, China), which promotes adhesion and electrical conductivity between aluminum foil and activated carbon film.

The procedure for electrode preparation is shown in Figure 1(a). First, the electrode paste was prepared by mixing activated carbon powders, conductive agent, and binder at the weight ratio of 90: 5: 5 in 1-methyl-2-pyrrolidinone (NMP). NMP was carefully added to adjust solid contents to be between 20 and 25 % by weight. A mixture was mixed using a vortex mixer for 15-30 min to achieve a homogeneously mixed carbon slurry. It can be noticed that a slurry flows similarly to thick honey. We report the viscosity test of our routinely formulated sample to be in the range of 3,000-5,000 cP (at the shear rate of 10 s^{-1}), and suggest the suitable viscosity range of 3,000-5,000 cP. It was noticed that if the viscosity value is over or under the proper range, it can cause peeling off or pinholes in an electrode. The carbon slurry was spread onto a sheet of current collector with a doctor blade device producing carbon film with the wet thickness of $250 \mu\text{m}$. A conductive-carbon coated aluminum foil was dried in an oven at $100 \text{ }^\circ\text{C}$ for 1 h. The dried electrode was transferred through a gap of calendaring rollers to achieve a dense and uniform-thickness electrode. Calendaring process was performed at room temperature with the determined gap size between $100 \mu\text{m}$ and $20 \mu\text{m}$.

2.2 Pouch cell assembly

The process diagram for pouch cell assembly is shown in Figure 1 (b) and the layout showing components of a supercapacitor pouch cell is illustrated in Figure 2. The capacitor consisted of two symmetric electrodes and a sheet of separators, in Figures 2(a) and 2(b), respectively. Single-side coated electrodes were cut to the predetermined size. A separator was placed between two electrodes and on the top of the upper electrode to prevent a short circuit. Two electrodes were aligned to maximize the overlapping area of carbon coating. A stack of electrode-separator, in Figure 2(c), was folded to minimize its size, as shown in Figure 2(d). Each electrode was attached with an aluminum strip to be utilized as an electrical terminal. Firm electrical contact can be achieved by welding or mounting two parts with a metal eyelet. The assembly of electrodes and separators was inserted into a pouch bag, as shown in Figure 2(e). A pouch was constructed from a $100\text{-}\mu\text{m}$ -thick aluminum laminated foil. It is noted that the thickness of a battery-grade laminated foil is typically $150 \mu\text{m}$ or thicker, in order to provide packaging toughness and durability. A cell contained pouch was heat sealed, leaving another end opened for electrolyte injection. It is suggested that hot melt adhesive must be applied to promote leak-free bonding between an aluminum terminal and laminated foil. The pouch cell was further dried in a vacuum oven at $100 \text{ }^\circ\text{C}$ for 1 h before transferred to a glove box for electrolyte injection. This drying step is to prevent contamination of moisture,

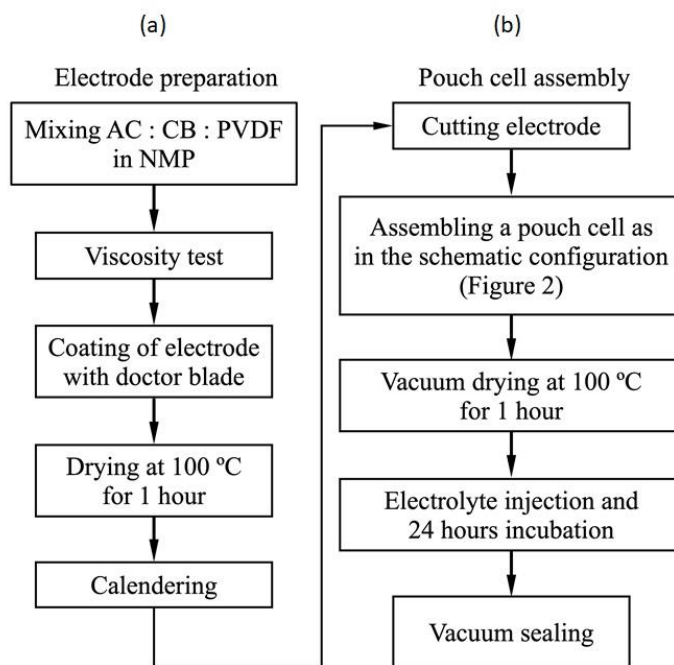


Figure 1. The flow chart of pouch cell supercapacitor fabrication: (a) electrode preparation and (b) pouch cell assembly

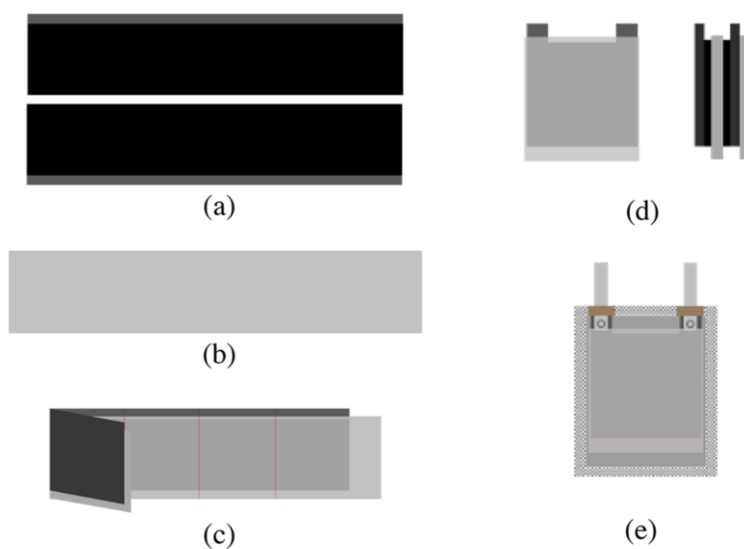


Figure 2. Layout showing components of a pouch cell supercapacitor: (a) carbon-coated electrodes, (b) a separator, (c) a stack of electrodes and separators, (d) front-view (left) and side-view (right) of a rolled cell, and (e) an assembled pouch cell

which typically causes electrolysis and deterioration of an electrode [13, 24]. In a glove box with a moisture level of less than 0.5 ppm, a pouch cell was then filled with an excess amount of electrolyte, approximately 5 ml, and sealed. In this study, 1M tetraethylammonium tetrafluoroborate (TEABF₄) in acetonitrile (ACN) or propylene carbonate (PC) was examined as organic electrolytes for a pouch cell supercapacitor. The sealed pouch cell was then incubated at room temperature for 24 h to allow impregnation of electrolyte. The pouch cell was finally vacuum sealed using a compact vacuum sealer and transferred out of a glove box for characterization.

2.3 Characterizations

Viscosity of a carbon slurry was measured in dynamic mode at the shear rate of 10 s⁻¹ and 19 °C using a Brookfield DV II+ viscometer with a SC4-29 spindle. Morphology of an electrode was investigated by using a Hitachi S3400N scanning electron microscope. For wettability test, a 5- μ l droplet of solvent, PC or ACN, was deposited on a sheet of separator, NKK or PP and observed by using a digital microscope, Dino-Lite Edge AM4815ZT, in order to measure the contact angle and estimate the capability of solvent absorption. In a study on calendaring condition, a Swagelok test cell was assembled from a pair of 10-mm diameter electrodes, a Whatman filter paper separator, and 1 M Na₂SO₄ aqueous electrolyte solution to evaluate the performance of a calendared electrode. All electrochemical measurements were performed using Autolab PGSTAT204 (Metrohm Autolab B.V., Switzerland). Cyclic voltammetry (CV) was performed at 3 mV/s within the potential range of 0 and 2.5 Volt. Galvanostatic charge-discharge (GCD) was performed in the same potential range at a charge-discharging current of 0.1 A/g. Capacitance and specific capacitance were calculated from the discharging curve of GCD. Cell resistance was calculated from voltage (IR) drop feature in GCD curve.

3. Results and Discussion

3.1 Pouch cell

Photographs in Figure 3 summarize fabrication of a pouch cell made of a 210-cm² supercapacitor electrode which contains the active material of approximately 1.2 g. Carbon electrode can be casted on an Al current collector manually using a doctor blade device, in Figure 3(a). The device is capable of coating the largest area of 7.5 cm \times 28 cm per batch, as shown in Figure 3(b). In order to make the electrode-separator stack more compact, the zig-zag folding is applied, as shown in Figure 3(c). After aluminum terminals are mounted to the electrodes using iron eyelets, a pre-fabricated cell is ready for pouch packaging, as shown in Figure 3(d). The complete pouch cell is shown in Figure 3(e). The pouch dimension was typically 7.5 \times 9 \times 0.25 cm³, while the size of stacked electrodes was 5.6 cm \times 3.8 cm. Some pouch cells may be swollen after long charge-discharge cycles, as shown in Figure 3(f). It is because moisture residue in a pouch provokes generation of gases or electrolysis products. Drying an assembly before loading into a glove box and vacuum sealing a pouch cell after electrolyte injection can reduce the remaining air and moisture inside a pouch cell. Therefore, these procedures must be applied to ensure a healthy pouch cell.

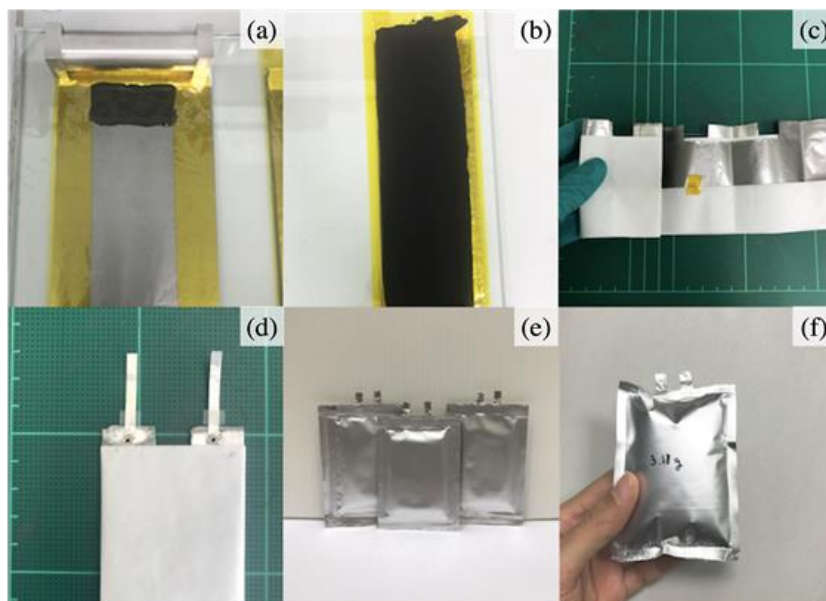


Figure 3. Photographs of an electrode (a) before and (b) after doctor blade coating of carbon slurry, (c) a stack of electrodes and a separator, (d) a rolled electrode assembly with aluminum terminals attached, (e) a sealed pouch cell, and (f) a swollen pouch cell.

3.2 Effects of calendaring

Calendaring, in principle, is a process to compress an electrode by passing a thick sheet of electrode through a slit of drum rollers, typically at elevated temperature. The compaction produces a flat surface, uniform thickness, and relatively dense carbon film. It promotes electrical contact between the electrode and current collector as well as activated carbon granules, which enhance conduction and accessibility of electrons throughout an electrode [16, 25]. Firm electrical contact results in increasing capacitance and reducing resistance.

In this study different calendaring conditions were tested on a sheet of supercapacitor electrode to determine the suitable electrode processing. The as-coated electrode was typically non-uniform thickness. After rolling pressed using the gap comparable to the electrode thickness, 80-100 μm , it appeared partially squeezed. Complete coverage of film compaction achieved at 60 μm gap and below. The cross-section SEM images of the electrode processed without calendaring, and calendaring with 60 μm or 50 μm gap are shown in Figures 4(a-c), respectively. The calendared electrodes exhibited uniform thickness and significant reduction in cavity compared with the as-coated electrode. Further calendaring with the smaller gap size showed no significant change in film morphology, and damages such as wrinkle on aluminum foil or peeled film started to be obviously seen. It was noticed that the thickness of the calendared electrode was greater than the gap size. The 60 μm and 50 μm calendared electrodes were measured to be 75 μm and 65 μm , respectively. It seems that the carbon electrode possesses spongy characteristic and there exists the saturated value density which may differ upon electrode materials and formulation. In the present work, the saturated density of the 90% activated carbon contained electrode is calculated to be approximately 0.7 g/cm^3 , while the thickness can vary with material loading.

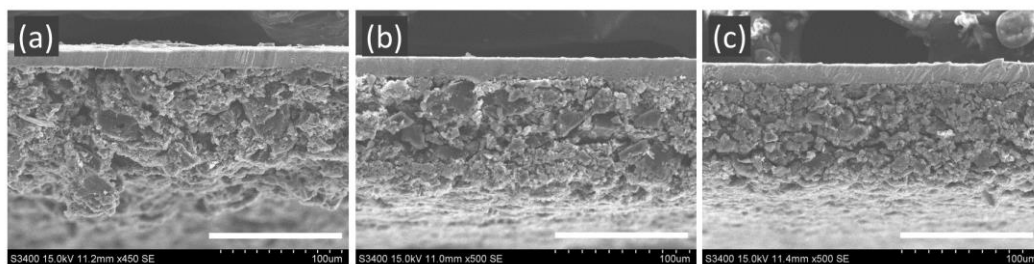


Figure 4. Cross-section SEM images of an electrode layer on aluminum foil (a) without calendaring and received calendaring with (b) 60 μm and (c) 50 μm gap; scale bars are 100 μm .

The aforementioned electrodes were further evaluated for capacitance using an aqueous electrolyte in a Swagelok test cell. Comparison of GCD of three test cells is shown in Figure 5. The specific capacitance of the control electrode, without calendaring, is 3.9 F/g. The IR drop was 70 mV, corresponding to the cell resistance of 30 Ω . For the calendared electrodes, the specific capacitance values were almost three times higher than the control electrode. They were 11.3 and 12.5 F/g for the 60 μm and 50 μm calendared electrodes, respectively. In addition, the IR drop of the calendared electrode was also relatively small. The IR drop values were 55 mV (21.5 Ω) and 42 mV (22 Ω) for the 60 μm and 50 μm calendared electrodes, respectively. There was a slight improvement in the capacitance with further calendaring. The maximum capacitance of 13.5 F/g was achieved for the case of 30 μm calendaring. The results suggest that adequate film compaction is crucial for the optimization of the electrode performance. Empirically, the 60 μm or 50 μm calendaring condition, which produces film compression of approximately 50% or greater, seems sufficient to take effect without the risk of electrode damage. As a consequence, we adopted 50 μm calendaring in procedure to make a pouch cell.

3.3 Selection of separators and solvents

Selection of separators and solvents was preliminarily examined by wettability test. Images of a solvent droplet on a separator for four solvent-separator combinations are illustrated in Figure 6. The PC droplet seems to stand on a PP sheet without being adsorbed, as shown in Figure 6(a). The contact angle was measured to be 75°. The result suggests that PC performs poor wetting on the PP separator. As a result, this solvent-separator combination was rejected from further investigation. The ACN initially formed a droplet on a PP sheet with the contact angle of 50°, in Figure 6(b). It was observed that ACN was gradually absorbed into a PP substrate, suggesting the moderate wettability of PP by ACN. In the case of the cellulose separator, both PC and ACN droplets were readily absorbed into the substrate, in Figures 6(c) and 6(d), indicating the excellent wettability of the cellulose separator by both solvents. Therefore, pouch cells based on the latter three solvent-separator system were fabricated to evaluate in the next step for electrochemical performance.

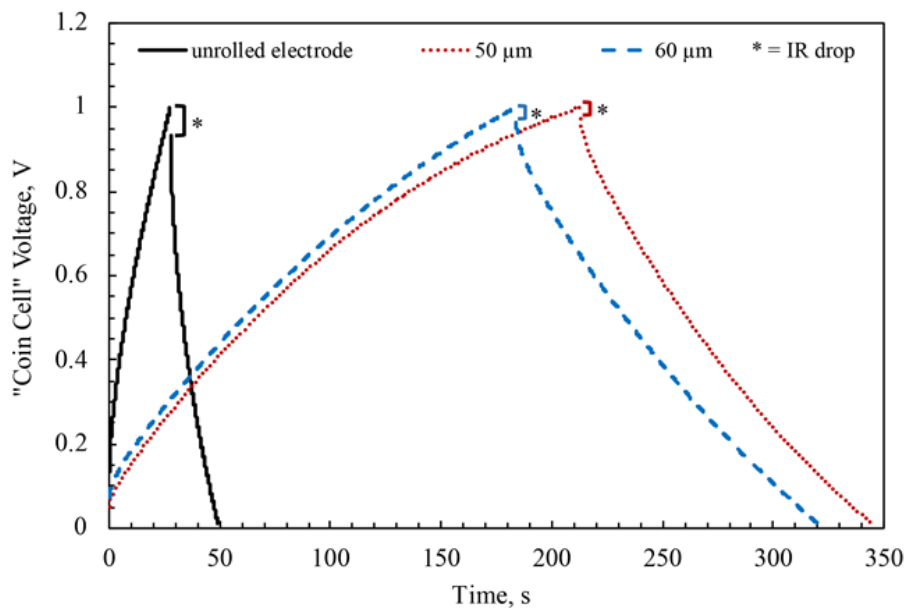


Figure 5. Comparison of GCD curves of coin cells fabricated without calendaring (unrolled), calendaring through 50 μm and 60 μm gaps; data were taken from the last charge-discharge curve of 5 cycles.

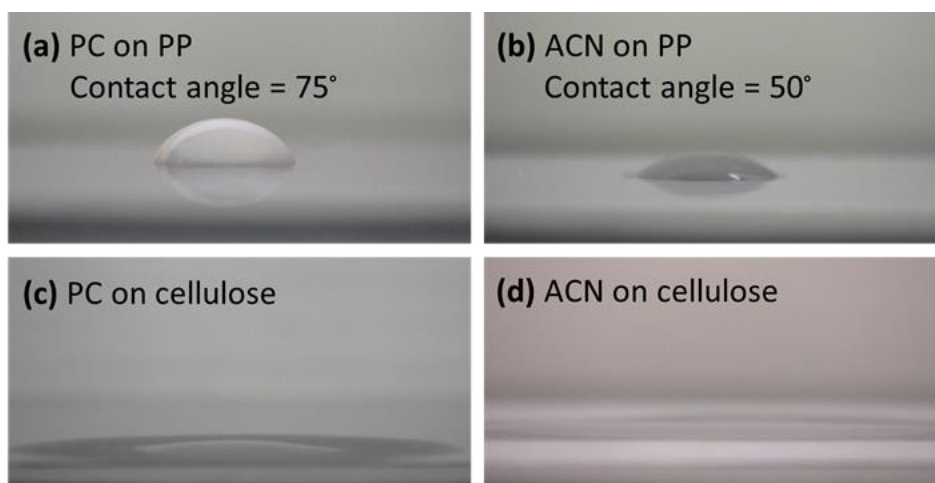


Figure 6. Photographs of a 5- μl droplet of (a) PC on PP, (b) ACN on PP, (c) PC on NKK cellulose, and (d) PC on NKK cellulose accompanied with the value of contact angle. A photograph was immediately captured after deposition of a droplet.

GCD curves of three pouch cells: a PP separator and 1M TEABF₄/ACN electrolyte (ACN-PP), an NKK cellulose separator and 1M TEABF₄/PC (PC-cellulose), and an NKK cellulose separator and 1M TEABF₄/ACN (ACN-cellulose) are presented in Figure 7. The ACN-PP shows the largest specific capacitances of 29.4 F/g and the smallest IR drop of 0.07 V, which is equivalent to the internal resistance of 0.3 Ω. The specific capacitance of the PC-cellulose and ACN-cellulose cells are 21.7 F/g and 26.3 F/g while the IR drop (internal resistance) values are 0.17 V (0.7 Ω) and 0.22 V (0.9 Ω), respectively. Although the cellulose possesses high porosity and the excellent wettability by the selected solvents which could promote ionic conductivity [13], it is found that the supercapacitor using the NKK cellulose separator tends to have less capacitance and relatively high internal resistance. As in our case the PP is thinner than the cellulose separator, one explanation could be the contribution from the thickness of a separator in which the thinner the separator is, the lower ionic resistance would be [12, 13]. Another explanation is that the hydrophilic nature and the high porosity of cellulose separator could provide rich interaction with the electrolyte solvent. Such interaction leads to swelling of the separator and a decline of cellulose mechanical strength after immersion in the electrolyte which may induce poor interfacial contact between an electrode and a separator, thus an increase in cell resistance [26]. In addition, ACN has a higher solvent reorganization energy compared to PC, which could cause additional ionic resistance in the case of the cellulose-solvent system.

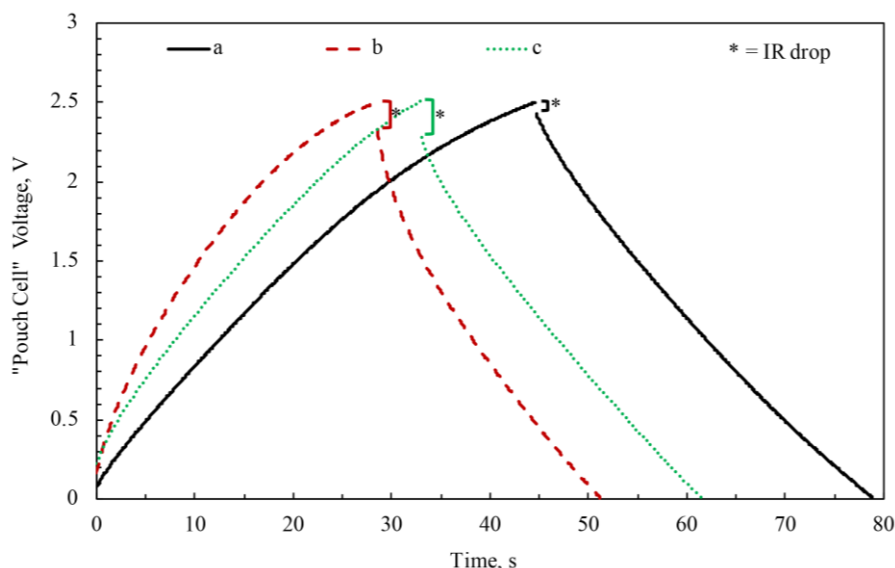
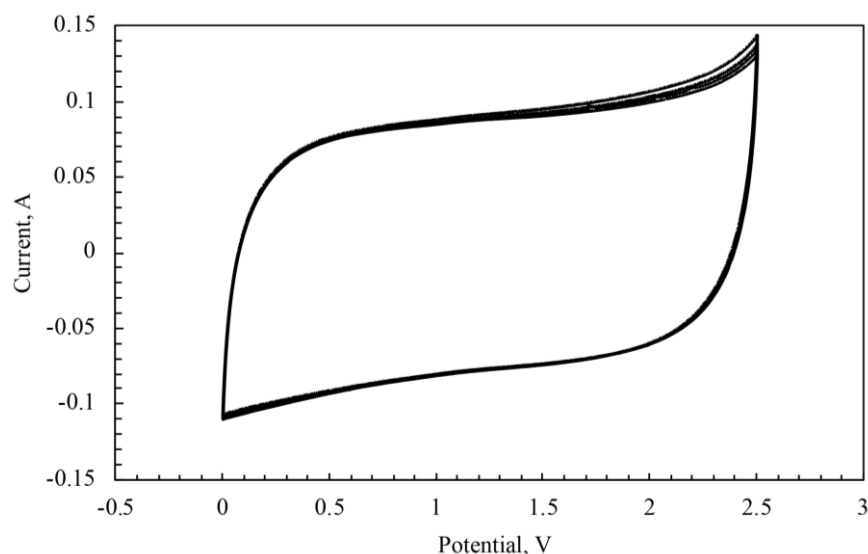


Figure 7. GCD curves of pouch cells with (a) PP separator in 1M TEABF₄/ACN, (b) cellulose separator in 1M TEABF₄/PC, and (c) cellulose separator in 1M TEABF₄/ACN

Under the scope of this study, it is suggested that ACN-PP is the best solvent-separator system for high capacitance application. The highest capacitance of 32.6 F was achieved in our optimized pouch cell. Summary of the optimized formulation and specification for the supercapacitor electrode are given in Table 1. The CV curve of a corresponding pouch cell supercapacitor is shown in Figure 8. The shape of the CV curve is almost rectangular which corresponds to the ideal EDLC in a potential range of 0 - 2.5 V. The steep tail at the upper-end potential suggests that the value of the rated voltage is limited to 2.5 V. This potential limit, rather than 2.7 V for a commercial cell, could be originated from the presence of moisture impurity.

Table 1. Formulation and specifications of an EDLC electrode in a pouch cell

Item	Both positive and negative electrode specification
Active material	90 wt.% activated carbon (TOB)
Conductive material	5 wt.% carbon black super-P (TOB)
Binder	5 wt.% polyvinylidene fluoride (PVdF: Sigma Aldrich)
Current collector	Conductive carbon coated aluminum foil (TOB)
Separator	Polypropylene (PP)
Electrolyte	1M TEABF ₄ /ACN
Electrode density	0.7 g/cm ³
Electrode porosity	65%

**Figure 8.** CV curve of pouch cell supercapacitor using electrode specified in Table 1

4. Conclusions

In this article, basic procedures to fabricate a pouch cell for a symmetric EDLC are described. Key material components and process steps are revealed, especially, the calendaring condition and the selection of separator-solvent combination have been highlighted. Detailed information provided here is aimed to encourage research community in the area of energy storage, to be capable of prototyping a large scale device and to close a gap between material research and application.

5. Acknowledgements

This project is supported by Energy Policy and Planning Office (EPPO), Ministry of Energy (Contract no. P-17-50509). Financial support from the Research Fund for DPST Graduate with First Placement (Grant no.27/2014) is also acknowledge. The authors would like to acknowledge EFS

scholarship from SIIT and the Center of Excellence in Materials and Plasma Technology, Thammasat University. Thanks to Dr. Prayoon Songsiriritthigul of the Suranaree University of Technology for helpful discussion and the Physical Characterization Laboratory, MTEC, for the support on viscosity measurement.

References

- [1] Al-Hallaj, S., Wilke, S. and Schweitzer, B., 2017. Energy storage systems for smart grid applications. In: A. Badran, S. Murad, E. Baydoun and N. Daghir, eds. *Water, Energy & Food Sustainability in the Middle East*. Cham, Switzerland: Springer.
- [2] Vazquez, S., Lukic, S.M., Galvan, E., Franquelo, L.G. and Carrasco, J.M., 2010. Energy storage systems for transport and grid applications. *IEEE Transactions on Industrial Electronics*, 57(12), 3881-3895.
- [3] Hannan, M.A., Hoque, M.M., Mohamed, A. and Ayob, A., 2017. Review of energy storage systems for electric vehicle applications: Issues and challenges. *Renewable and Sustainable Energy Reviews*, 69, 771-789.
- [4] Horn, M., MacLeod, J., Liu, M., Webb, J. and Motta, N., 2019. Supercapacitors: A new source of power for electric cars?. *Economic Analysis and Policy*, 61, 93-103.
- [5] Mejdoubi, A.E., Chaoui, H., Gualous, H., Oukaour, A., Slamani, Y. and Sabor, J., 2016. Supercapacitors state-of-health diagnosis for electric vehicle applications. *World Electric Vehicle Journal*, 8(2), 379-387.
- [6] Muyeen, S.M., Shishido, S., Ali, M.H., Takahashi, R., Murata T. and Tamura, J., 2007. Application of energy capacitor system to wind power generation. *Wind Energy*, 11(4), 335-350.
- [7] Maxwell Technologies. *Document number: 3000615-EN.2*. [online] Available at: https://www.maxwell.com/images/documents/Ultracapacitors_Overview_Flyer_3000615-2EN.pdf
- [8] Soltani, M., Ronsmans, J., Kakihara, S., Jaguemont, J., Bossche, P.V., Mierlo, J. and Omar, N., 2018. Hybrid battery/lithium-ion capacitor energy storage system for a pure electric bus for an urban transportation application. *Applied Sciences*, 8, 1176.
- [9] Iro, S.Z., Subramani, C. and Dash, S.S., 2016. A brief review on electrode materials for supercapacitor. *International Journal of Electrochemical Science*, 11, 10628-10643.
- [10] Pandolfo, A.G., Wilson, G.J., Huynh, T.D. and Hollenkamp, A.F., 2010. The influence of conductive additives and inter-particle voids in carbon EDLC electrodes. *Fuel Cells*, 10(5), 856-864.
- [11] Böckenfeld, N., Jeong, S.S., Winter, M., Passerini, S. and Balducci, A., 2013. Natural, cheap and environmentally friendly binder for supercapacitors. *Journal of Power Sources*, 221, 14-20.
- [12] Zhong, C., Deng, Y., Hu, W., Qiao, J., Zhang, L. and Zhang, J., 2015. A review of electrolyte materials and compositions for electrochemical supercapacitors. *Chemical Society Reviews*, 44, 7484-7539.
- [13] Zhong, C., Deng, Y., Hu, W., Sun, D., Han, X., Qiao, J. and Zhang, J., 2016. Compatibility of Electrolytes with Inactive Components of Electrochemical Supercapacitors. In: *Electrolytes for Electrochemical Supercapacitors*. [online] Available at: <https://www.routledgehandbooks.com/doi/10.1201/b21497-4>
- [14] Arora, P. and Zhang, Z., 2004. Battery separators. *Chemical Reviews*, 104, 4419-4462.
- [15] Liu, X., Dai, X., Wei, G., Xi, Y., Pang, M., Izotov, V., Klyui, N., Havrykov, D., Ji, Y., Guo, Q. and Han, W., 2017. Experimental and theoretical studies of nonlinear dependence of the

- internal resistance and electrode thickness for high performance supercapacitor. *Scientific Reports*, 7, 45934.
- [16] Dsoke, S., Tian, X., Täubert, C., Schlüter, S. and Wohlfahrt-Mehrens, M., 2013. Strategies to reduce the resistance sources on electrochemical double layer capacitor electrodes. *Journal of Power Sources*, 238, 422-429.
- [17] Bhattacharjya, D., Carriazo D, Ajuria, J. and Villaverde, A., 2019, Study of electrode processing and cell assembly for the optimized performance of supercapacitor in pouch cell configuration. *Journal of Power Sources*, 439, 227106.
- [18] Masarapu, C., Wang, L.P., Li, X. and Wei, B., 2012. Tailoring electrode/electrolyte interfacial properties in flexible supercapacitors by applying pressure. *Advanced Energy Materials*, 2, 546-552.
- [19] Roberts, A.J., 2019. Effect of time, temperature and potential on pre-conditioning of supercapacitors. In: *ECS Meeting Abstract*, The Electrochemical Society, p. 116.
- [20] Roberts, A.J., Rubio, I., Gonzalez, D. and Bhagata, R., 2016. Supercapacitors: From coin cell to 800 F pouch cell. In: *ECS Meeting Abstract*, The Electrochemical Society, p. 1029.
- [21] Rubio, I., Gonzalez, D., Stoevab, Z., Lowa, J.C.T. and Roberts, A.J., 2017. Development and Testing of Large Format Graphene Supercapacitors, in: *Meeting Abstract*, The Electrochemical Society, p. 595.
- [22] Azais, P., Tamic, L., Huitric, A., Paulais, F. and Rohel, X., 2016. *Separator Film, Its Fabrication Method, Supercapacitor, Battery and Capacitor Provided with Said Film*, US. Pat. 9,461,288.
- [23] Xiamen Tob New Energy Technology Co., Ltd. *Specifications: 25um PP Film Battery Separator for Lithium Battery Research*. [online] Available at: <https://tob.en.alibaba.com>
- [24] Morita, M., Noguchi, Y., Tokita, M., Yoshimoto, N., Fujii, K. and Utsunomiya, T., 2016. Influences of residual water in high specific surface area carbon on the capacitor performances in an organic electrolyte solution. *Electrochimica Acta*, 206, 427-431.
- [25] Haselrieder, W., Ivanov, S., Christen, D.K., Bockholt, H. and Kwade, A., 2012. Impact of the calendaring process on the interfacial structure and the related electrochemical performance of secondary lithium-ion batteries. *ECS Transactions*, 50(26), 59-70.
- [26] Liu, W., Dang, Y., Xie, W. and Tang, A., 2019. Weakening of mechanical properties of cellulose separator caused by electrolyte immersion and elevated temperature. *Polymer Composites*, 40(10), 3857-3865.